Gasification and structural behaviour of different carbon sources and resultant chars from rapid devolatilization for HIsarna alternative ironmaking process

Darbaz Khasraw [a,*], Theint Theint Htet [a], Xinliang Yang[a], Volkan Degirmenci [b], Hans Hage [c], Koen Meijer [c], Zushu Li [a,*]

[a] **WMG, University of Warwick, Coventry CV4 7AL, UK**

[b] **School of Engineering, University of Warwick, Coventry CV4 7AL, UK**

[c] **IJmuiden Technology Centre, PO Box 10000, 1970 CA IJmuiden, The Netherlands**

Abstract: To evaluate the potential of using renewable biomass in the novel HIsarna technology, reactivity of thermal coal (TC), charcoal (CC), Bana grass char (BGC) before and after rapid devolatilization at 1500 °C in a drop tube furnace (DTF) was investigated. Thermogravimetric (TG) was used for CO_2 gasification study, and high temperature confocal scanning laser microscope (HT-CSLM), Brunauer-Emmett-Teller (BET) and scanning electron microscopy (SEM) were used to characterise the morphology of all three raw carbonaceous materials and their chars produced by rapid devolatilization. CC has fastest gasification reaction before and after rapid heat treatment, and BGC raw is more reactive than TC raw but BGC 1500 °C and TC 1500 °C have very similar gasification behaviour. The reactivity index of the rapidly devolatilized char is reduced to 84.21% (BGC), 92.11% (TC) and 94.23% (CC) compared to their raw materials. This shows that BGC is more severely affected by the rapid devolatilization, and this behaviour is likely to be governed by the high ash content which will melt and cause pore blockage during heat treatment. According to HT-CSLM results the average particle sizes decreased by 28%, 24% and 20 % for TC, CC and BGC respectively. While the SEM images shown that TC has gone through significant structural changes during the rapid devolatilization, but CC and BGC maintained their parent structural shapes. The BET results indicate that TC is non-porous,

but both CC and BGC contain a large number of constricted micropores with significantly larger surface area.

Keywords:
HIsarna technology
Coal and biomass chars
Rapid devolatilization
Reactivity
Drop tube furnace (DTF)
Thermogravimetric analysis (TGA)

* Corresponding author. Tel.: +44 (0)24 7652 4706;
E-mail address: d.khasraw@warwick.ac.uk (D. Khasraw)
E-mail address: z.li.19@warwick.ac.uk (Z. Li)
Postal address: WMG, University of Warwick, Coventry CV4 7AL, UK

1. Introduction

The HIsarna process is developed under the European Ultra-Low CO_2 Steelmaking (ULCOS) programme as an alternative to the conventional blast furnace ironmaking due to concerns about global warming and climate change [1]. HIsarna combines the cyclone converter furnace (CCF) and the smelting reduction vessel (SRV) into a single highly integrated smelting furnace to operate as shown in Figure 1. A pilot plant with the production capacity of 8 ton/hr hot metal was built in Tata Steel IJmuiden in 2010, subsequently commissioned and first test campaign took place in 2011 [2], [3]. During the experimental campaigns a wide range of raw materials has been investigated confirming high flexibility on the raw materials [4]. HIsarna can operate with thermal coal and fine ore directly, therefore coke making and sinter plants are not required, which results in a reduction of CO_2 emission by 10-20 % or potentially more than 80 % with the addition of carbon capture and storage (CCS)

compared with the conventional blast furnace ironmaking process [5]. In addition, the raw material flexibility also creates an opportunity to utilise renewable fuels including biomass and still maintain process efficiency.

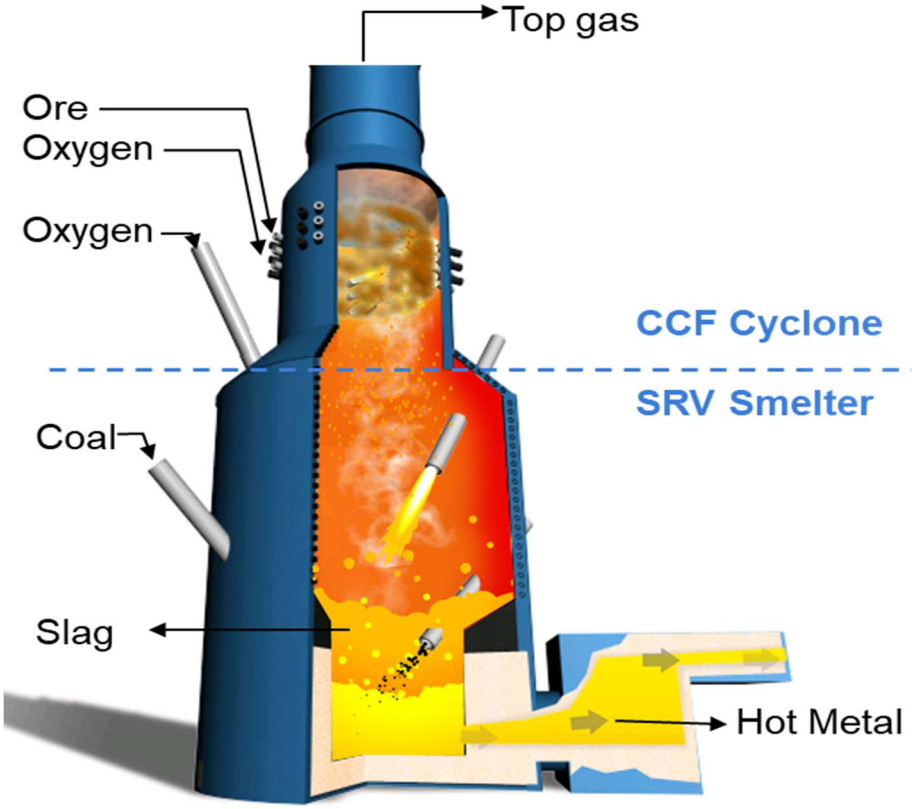

Figure 1. A schematic of HIsarna technology combines CCF and SRV [6] .

HIsarna starts with iron ore, fluxing materials and oxygen injected into the CCF, where CO rich off-gas evolved from the SRV is burning and reacting with the ore. According to Chen et al., the reacting gas temperature in the cyclone can reach the temperature between 1400-2000 °C [7]. As a result the iron ore fines are melted and pre-reduced by up to 20%, through thermal decomposition and reduction by the post-combustion gases arising from the SRV [8], [9]. After hitting the wall of the cyclone, molten iron ore moves down under gravity into the slag layer in the SRV where the temperature is between 1400-1500 °C. The granular coal (or other carbonaceous materials) is injected into this slag layer to fully reduce the iron ore to hot metal and to dissolve carbon into the hot metal to compensate carbon used in smelting reduction steps [2].

The carbonaceous materials injected are subjected to a series of rapid physical and chemical changes including rapid heating (from ambient temperature to 1500 °C) and devolatilization. Depending on the ultimate temperature and the heating rate the devolatilization process can finish within several milliseconds under rapid heating or several hours under slow heating [10]. Devolatilization is the first step of all the thermochemical processes, and it comprises the release of volatile matter and change in the solid structure due to occurrence of different phenomena such as softening, swelling, fragmentation [11], [12]. Due to the extreme high temperature (up to 1500 °C) in SRV, a large amount of volatiles are released instantly after injection of carbonaceous materials which results in dramatic transformation in the solid particle structure. The ascending hot gas stream created by the released volatiles during devolatilization, and the gases generated by reactions within the SRV will maintain the temperature in the CCF and partially reduce the iron oxide. However, about 80% of the reduction reactions takes place in the SRV, through direct/indirect reactions between FeO in slag with solid char, dissolved carbon in the liquid metal and reducing gases respectively. The overall reaction between FeO containing slag and solid carbon or carbon in molten iron at high temperatures can be described by equation (1).

$$FeO_{(l)} + C_{(s)} / [Fe–C_{(l)}] \rightarrow Fe_{(l)} + CO_{(g)} \quad (1)$$

Previous studies have shown that parameters including particle size, surface roughness, shape, porosity and chemical composition of the char as well as the reaction atmosphere affect the reduction of FeO in the slag and dissolution of carbon in the metal bath [13]–[18]. It was found that the ultimate structure will have a significant effect on the wetting and the contact angle between materials, which subsequently affects the reactivity of the char and will influence the reduction rate of FeO in the slag through direct/ indirect reactions. It is well known that thermal treatment significantly affects the final char morphology of the carbon material, therefore an extreme high temperature in SRV will have a significant impact on the char structure e.g. shape, size, roughness and porosity [12], [19]–[21]. Therefore, to select the right mix of carbonaceous materials such as replacing thermal coal with biomass, it is essential to understand the changes in the char morphology and reactivity and the

formation of char structure for each carbonaceous material caused by the rapid devolatilization under thermal conditions similar to the HIsarna SRV, that is, High-temperature and rapid heating.

Effects of experimental conditions such as temperature, heating rate, pressure, residence time and reaction atmosphere on physical and chemical properties of chars produced from coal and biomass materials have been extensively investigated [12], [19], [28]–[31], [20]–[27]. These studies are carried out through evaluating the char morphology and size changes caused by the variation of these conditions, as well as the kinetics and char reactivity analysis under different oxidation conditions. Through examining the size and morphology of two biomass materials and chars produced under rapid heating to 1400 °C by Biagini et al. [21], it was revealed that the rapid heating caused significant structural variations in the chars produced in respect to the parent materials. The study also found that the char particle size reduced quite significantly by rapid heating for woody biomass, however the change in size was negligible for olive char. In another study by Biagini et al., it was found that the particle size for all the fuels decreases with severe heating and also the density of coal decreases, but the density of biomass fuels increases [31]. During the investigation of porous structure parameters for different grades of coal to compare with biomass char produced at high temperature by Smoliński and Howaniec, it was found that the micro pore surface, area and volume of carbonaceous materials depend on the chemical properties, therefore an increase in the fixed carbon content will result in decrease in the porous structure of the material [22]. Biagini et al. [12] also studied the reactivity of char residues remaining from the rapid heating of two biomass materials to different final temperatures and concluded that the chars produced under higher temperatures are more reactive to air oxidation atmosphere than chars produced in milder conditions. The kinetic study carried out by Tanner and Bhattacharya using different oxidation atmospheres showed that the gasification atmosphere can affect the kinetic parameters but the particle size selected did not have big influence on the reaction kinetics [23]. Karlström et al. [24] studied the apparent reaction order for different coals and a biomass, and concluded that depending on the operating conditions, the reaction order can vary for carbonaceous materials and the study showed higher reactivity for biomass char compared to coal.

Moreover, other factors such as biomass torrefaction degree [25], particle size [26], and residence time [27], are shown to have an impact on the reactivity of the chars produced by high-temperature rapid devolatilization.

Although extensive research has been conducted on char characterization for different carbonaceous materials, the research reported was mostly carried out under low or medium temperature up to 1000 °C and focused on the properties of the chars and not much detailed explanation was given on how these properties may affect the utilization of char in ironmaking processes. To understand characteristics of the chars received in the SRV bath, the study of these materials needs to be undertaken under more extreme conditions similar to SRV e.g., higher heating rate and temperature, and investigate the implication of the char properties on the SRV behaviour. Therefore, the objective of this study is to investigate coal and biomass char particles produced under similar thermal conditions to the HIsarna's SRV. To simulate the sudden high heating rate and high temperature conditions that the carbonaceous materials experience, a drop tube furnace reactor (DTF) is used to produce char particles. The resultant chars are subsequently used for morphology, image analysis and reactivity test using SEM imaging, ImageJ software and thermogravimetric analyser (TGA) respectively. Also, the high temperature confocal scanning laser microscope (HT-CSLM) is used to monitor the real-time changes of carbonaceous particles during rapid heating. The HT-CSLM allows for continuous imaging of 2D plane within the small sample surface, to observe changes in size and shape of the particles under controlled high heating and cooling conditions applied.

2. Materials and methods

2.1. Sample preparation

One thermal coal and two biomass samples were chosen for this study. All the samples were dried at 80 °C for 12 hours to ensure all the surface moisture has been removed, and then crushed into small particles with the size range from 90 to 300 µm. The thermal coal (TC) and charcoal (CC) (a Birch wood based pre-treated biomass) have already been used in HIsarna process during the pilot plant trials, while the Bana grass char (BGC) (derived from a grass-based torrefied material provided by Orange –

Green through Tata Steel Nederland) is another renewable biomass source which may be considered for future HIsarna trials. Table 1 shows the proximate and ultimate analysis data for all three samples.

Table 1. Proximate and ultimate values of the used carbonaceous materials using ISO 17246:2010 standards

	TC	CC	BGC
Proximate Analysis wt% (db)			
Moisture/ % (ad)	8.87	4.56	2.52
Volatile Matter	22.18	12.10	19.00
Ash	8.80	1.80	9.11
Fixed Carbon (by difference)	69.02	86.10	71.89
Ultimate Analysis wt% (db)			
Carbon	81.91	89.40	78.60
Hydrogen	4.27	3.11	3.28
Nitrogen	2.19	0.57	0.46
Sulphur	0.24	0.06	0.14
Oxygen by (difference)	2.59	5.06	8.41

db – dry basis; ad – air dried.

2.2. Experimental methods

2.2.1. High temperature char preparation

The high temperature chars are produced through rapid devolatilization of the carbonaceous materials in the drop tube furnace (DTF) which is schematically shown in Figure 2. The DTF is constructed using an electric resistance heating high temperature vertical tube furnace (VTF) with a recrystallized alumina tube (VTF-1700/50, internal diameter 88 mm x length 1000 mm) and an isothermal reaction zone (±5 °C) of 250 mm. Before injecting the sample particles, the furnace was heated to the pre-set temperature of 1500 °C, allowing the carbon samples injected to be rapidly heated at the heating rate of approximately 10^4–10^5 °C/s [20]. The carbon particles were injected into

157 the pre-set temperature zone through a particle feeder designed using a tee piece connected to two
158 ball valves and an argon line to create an inert atmosphere and carry the particles to reaction zone
159 during injection as shown in Figure 2. The particle feeder was mounted to the top water-cooled flange
160 and directly connected to an alumina lance (internal diameter 5 mm) inserted through the flange into
161 the reactors hot zone. Before the experiment starts a sample of approximately 100 mg was placed on
162 the seat of the bottom ball valve on the “off” position, and Ar (with a 99.999% purity) flush through
163 the feeder to create an oxygen-free atmosphere and then closed all the valves. While the furnace was
164 heated to the desired temperature at the heating rate of 10 °C/min, a carrier gas (Ar, 99.999% purity)
165 controlled at 1 L/min was purged through the furnace from the bottom to ensure an inert atmosphere.

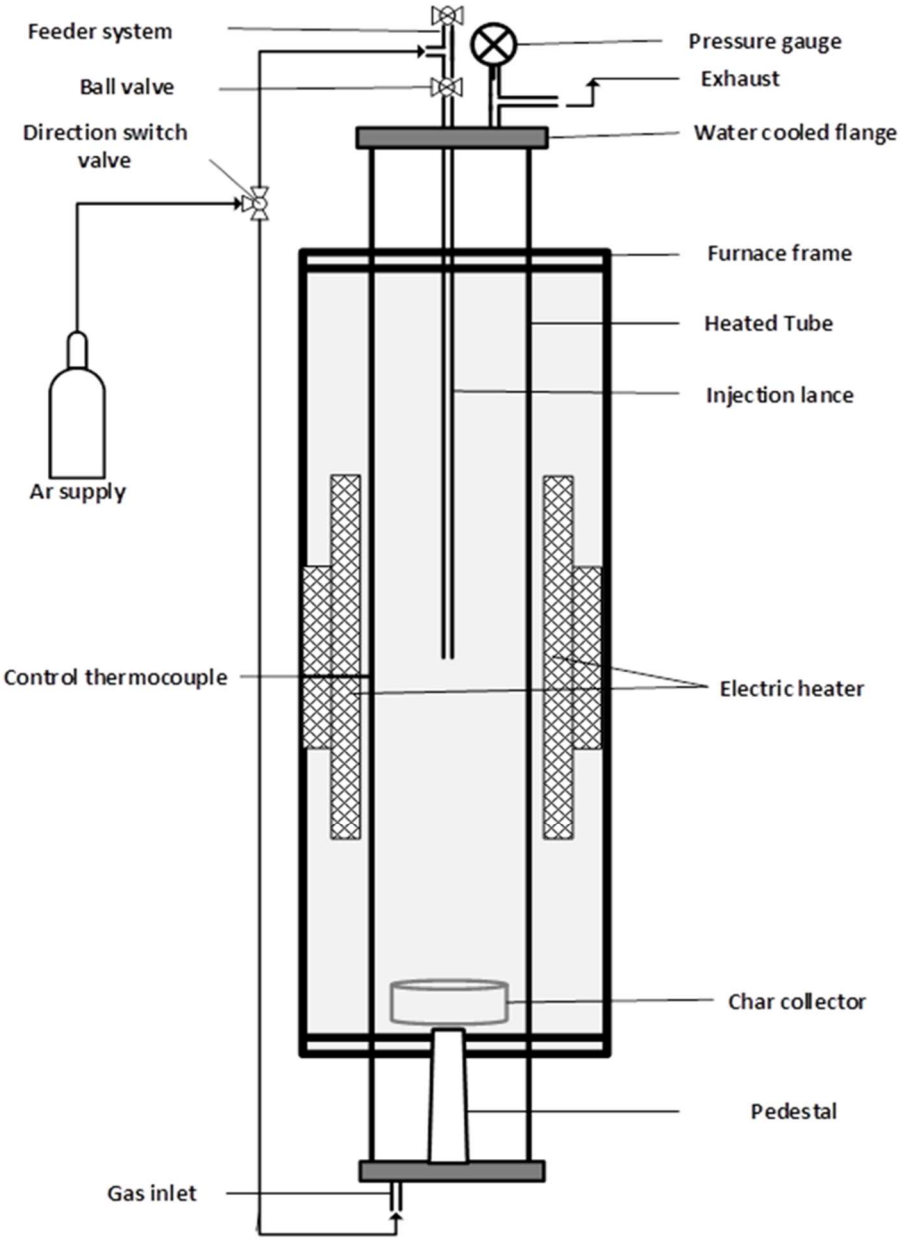

166

167 *Figure 2. Drop tube furnace (DTF) for rapid devolatilization study to produce solid char particles.*

168 When the furnace temperature reached the pre-determined high temperature, the valve holding the
169 sample was opened, and at the same time the valve controlling the Ar gas was switched to the feeder
170 for ~10 seconds to maintain the atmosphere while the samples are injected and carry the sample
171 particles to the isothermal region in the furnace and collected in the crucible at the bottom of the
172 furnace.

173 The ash tracer method was used to determine the char yield for each carbonaceous material during
174 the rapid heat treatment, assuming the minimum mass remaining after combustion is the ash content

175 of the samples. The ash tracer method assumes that ash is an inert material and maintained during
176 combustion process [32]. One gram of dried materials for each raw carbon source and their
177 devolatilized chars are added to pre-weighted alumina boat and placed in the muffle furnaces under
178 air atmosphere. The samples are heated at the heating rate of 10 °C/min, and then held at 800 °C for
179 an hour to ensure that the combustion process is completed. The sample remaining and pre-weighted
180 alumina boat are weighed again, then the initial alumina boat weight subtracted to obtain the weight
181 of the ash, and using equation (2) below the char yield was calculated [33]:

182 $$Char\ yield\ \% = \frac{Ai}{Ac}\ x100 \qquad (2)$$

183 Where *Ai* is the ash content in the raw carbonaceous material (on a dry basis) and *Ac* is the ash content
184 in the char produced under HIsarna thermal condition (on a dry basis).

185 **2.2.2. Analytical method for char characterization**

186 Char particles produced during DTF injection in 2.2.1 and parent materials are analysed and compared.
187 The reactivity test for the char particles was carried out using thermogravimetric analysis (TGA) with
188 a NETZSCH STA 449 instrument that has an analytical balance sensitivity of ± 0.01 mg. A 20 mg ± 0.01
189 sample was placed in an alumina crucible (height 4 mm x diameter 6.8 mm). The alumina crucible with
190 test sample was placed on a platinum stage, which has a thermocouple located directly underneath
191 to provide real temperature for the sample tested. All the samples were heated from the ambient
192 temperature to 1500 °C at the heating rate of 30 °C/min in a high purity (99.9999%) argon atmosphere
193 with the flow rate of 50 ml/min. Once the desired temperature reached the sample was kept at that
194 temperature for 10 minutes under Ar and then the gas atmosphere switched to (99.999%) CO_2 for 30
195 minutes with the flowrate of 50 ml/min to minimize the resistance around the particles resulting from
196 the stagnant gaseous film. The mass loss of the sample was continuously recorded to analyse the
197 effect of rapid heat treatment on each carbonaceous material in comparison to their parent materials.
198 The test samples are subject to buoyancy effects, therefore, to eliminate the errors caused by these
199 effects, the correction measurements were carried out by filling alumina crucibles with 20mg of inert
200 Al_2O_3 powder and perform similar test procedures to actual test samples, then the results of the inert

tests were subtracted from the test results. To ensure the reliability and reproducibility of the method, the test for the same sample has been repeated three times to produce concordant results. The gasification test results are used to calculate parameter such as char conversion and reactivity index for each material. Carbon conversion due to gasification is defined by equation (3):

$$X = \frac{mi - mt}{mi - mf} \quad (3)$$

where mi is the initial weight of the sample before gas atmosphere was changed to CO_2, mt is the instant weight of the sample at time t, and mf is the final weight of the sample after gasification reaction. The gasification reactivity is evaluated by the reactivity index ($R_{0.5}$) which is expressed by equation (4).

$$R_{0.5} = \frac{0.5}{t_{0.5}} \quad (4)$$

where $t_{0.5}$ is the time when char conversion is 50%.

2.2.3 Char structure analysis

Scanning electron microscopy (Sigma Zeiss SEM) images were obtained for each carbonaceous material sample before and after rapid heat treatment to investigate changes in shape and structure. Some random particles of each material were mounted to the carbon stub and placed in the SEM chamber. Magnification degree between 200 X to 400 X with the imaging conditions of 10 kV voltage applied for detailed study of SEM images for single particles e.g., surface roughness and porosity.

N_2 (77K) adsorption was applied to determine the carbonaceous material specific surface area, pore volume, and average pore diameter based on the multipoint Brunauer-Emmett-Teller (BET) method [22]. Approximately 1g of both raw and char samples for each carbonaceous material was degassed by heating at 200 °C under vacuum for 12 hours. Then using BET equipment (Micromeritics ASAP2020) the N_2 adsorption isotherms were obtained at liquid nitrogen temperature (77 K) and relative pressures between 0.011 and 0.996 for the degassed sample.

2.2.4. Direct observation under high temperature confocal scanning laser microscope (HT- CSLM)

The schematic of the HT-CSLM microscope is shown in Figure 3. The inner body of the chamber is a gold-coated, elliptical shape, to provide reflection for the IR radiation produced by the halogen lamp at the lower focus point to heat the small sample at the upper focus point. This results in possible heating rates of up to 1000 °C/min and temperatures up to 1600 °C. The platinum sample holder is positioned in the centre of the upper focal point through the extension of an alumina rod from the side of the chamber. A R-type thermocouple wire is fused into the bottom of the platinum sample holder at the free end of the alumina rod to provide real temperature of the samples tested. A small quantity of dispersed particles from each carbon source was added into the Pt crucible (height 4 mm x diameter 6.5 mm). The Pt crucible with the test sample was placed on alumina (Al_2O_3) spacer on the platinum stage within the reaction chamber, the alumina spacer is used to prevent fusing between Pt crucible and the platinum stage at high temperatures.

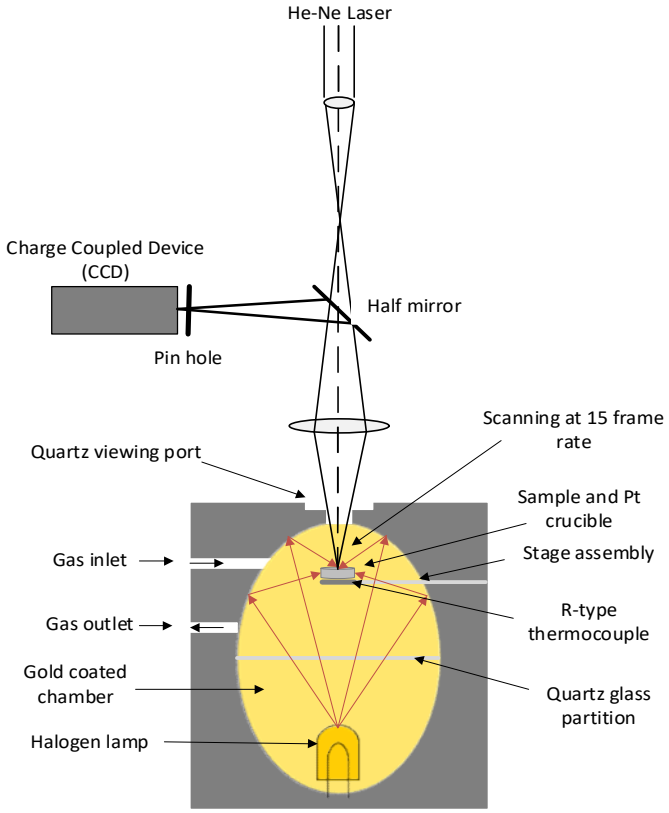

Figure 3. Schematic of the HT-CSLM to study real-time changes in the shape of carbon particles

Before starting experiments, the chamber was evacuated using rotary vacuum pump for a few seconds and being refilled with a high purity (99.9999%) argon gas. This procedure was repeated three times

to ensure an inert gas atmosphere achieved. The experiments were then performed under continuous argon flow of 300 ml/min to remove volatiles released by the sample and maintain an inert atmosphere within the reaction chamber. The furnace was first heated from the atmospheric temperature to 200 °C, at the heating rate of 60 °C/min and held at that temperature for 60 seconds to dry the samples, to condition the bulb and evaporate isopropanol which was used for cleaning. Then the sample was heated to 1000 °C at the heating rate of 100 °C/min, to ensure the sample is devolatilized and clear images are captured to measure all the changes in the particle structure. Using an X5 objective lens the optical system positioned directly above the heating chamber was set to simultaneously record 2D plane images at a rate of 15 frames per second, which can be viewed as either a video or still images. Using ImageJ software, the change in the particle size was measured in terms of their 2D area at different temperatures. These measured areas were then used to calculate the swelling ratio of the particle at temperature (SR_t) which is defined by Equation (5) where A_0 is the area of the particle at the beginning of the test and A_t is the area of the particle at temperature = t.

$$SR_t = \frac{A_t}{A_0} \quad (5)$$

To ensure representative results are produced, five particles in each sample were focused on and the changes in particle shape and size at different temperatures were measured to calculate mean particle change.

3. Results and discussion

3.1. Devolatilization results

To investigate the effect of rapid heating and high temperature devolatilization on carbonaceous materials and determine the difference in the behaviours of these three materials, DTF was used to produce chars. The produced char particles were considered to have similar physical and chemical properties to those encountered in the HIsarna process. During the rapid heating of carbonaceous materials several reactions take place simultaneously, including break-up of chemical bonds, vaporization, and condensation. The moisture and volatile matter content decreased significantly because of the effect of high temperature, while the fixed carbon increased resulting from the

vaporisation of the moisture and the release of the volatile matter. Using the ash tracer method, the char yield for TC, CC and BGC was calculated as 78.0 %, 69.9% and 80.2% respectively. This indicates that CC has gone through the highest conversion degree (30.1%), followed by TC (22.0%) and BGC (19.8%) which has lowest conversion degree during injection. According to the proximate analysis results CC has the lowest volatile matter content with the highest fixed carbon, yet the conversion degree was the highest, which indicates that oxidation of the carbon was most significant for CC during injection. These results agreed with the authors' previous findings using different techniques to measure the char yield for two of these materials [33]. The char yield was calculated by weighing the carbonaceous material before and after the rapid heat treatment at the temperatures of 1000, 1250 and 1500 °C and the weight loss results are very similar in this study compared to previous finding for both TC and CC at 1500 °C [34].

On the other hand, the conversion of both TC and BGC was much lower than CC and the conversion due to rapid devolatilization agrees with the volatile matter content in their raw materials. This behaviour for CC confirms that injection of CC can lead to lower char yield in HIsarna's SRV bath compared to TC and BGC, but higher combustible gas yield which could affect the HIsarna reactors behaviour. For example, it may be necessary to increase the HIsarna's CCF efficiency (i.e., the efficiency of iron pre-reduction in CCF by CO off-gas evolved from the SRV) to utilise the extra reductive gas proportion produced during CC injection to maintain the overall efficiency for combination of CCF and SRV. Furthermore, the results reveal that despite the lower VM content in CC, its conversion is significantly higher, therefore the char yield is not determined by VM content only, but also the physical and chemical properties of carbonaceous materials directly influence the solid char yield during rapid devolatilization.

3.2. Gasification analysis using Thermogravimetric analyser (TGA)

To compare the gasification behaviour of the carbonaceous materials selected and study the effect of rapid devolatilization, the reactivity with CO_2 is analysed using TGA for the char particles produced during DTF injection and their parent materials. The relative reactivity of the three carbonaceous

materials and their chars prepared under rapid devolatilization are compared using their weight-loss profile in TGA, as shown in Figure 4.

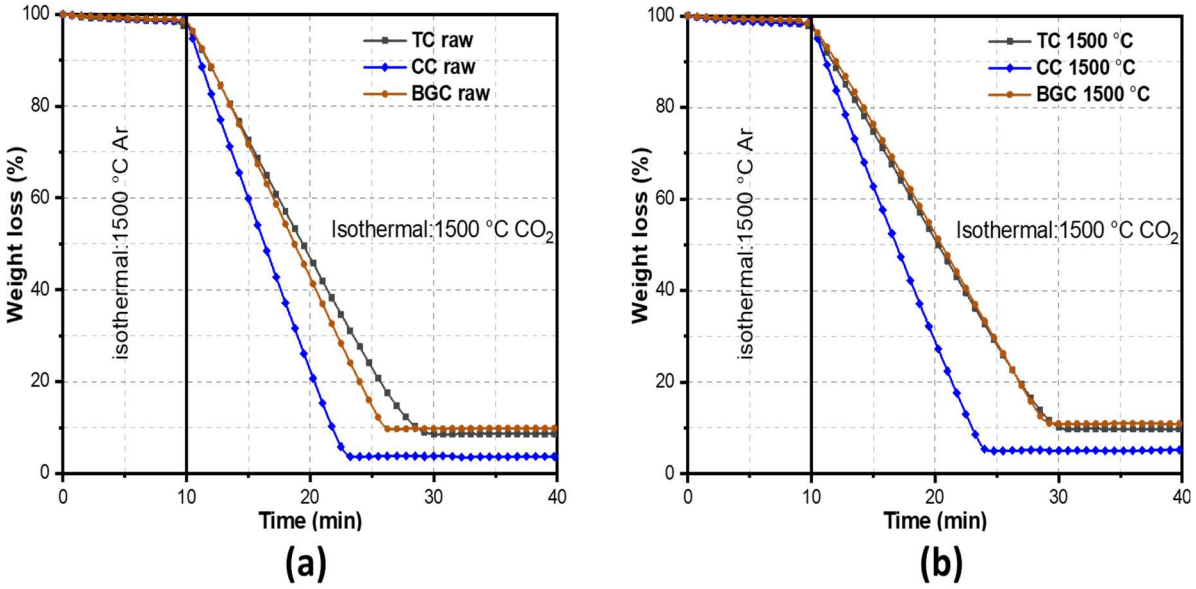

Figure 4. The isothermal weight loss profile under carbon dioxide at 1500 °C for (a) raw carbonaceous materials and (b) chars produced during rapid devolatilization in the DTF.

Clearly, the raw CC has the fastest gasification reaction with CO_2, followed by the BGC raw and TC raw (Figure 4a). The CC char produced from rapid devolatilization has the fastest gasification reaction with CO_2, but the BGC and TC chars produced from rapid devolatilization showed very similar behaviour as can be seen in Figure 4b. Based on this weight loss profile, the reactivity index values with the error bars representing standard error in either side of the mean are calculated and shown in Figure 5. As shown in Fig. 5, rapid devolatilization causes the carbonaceous materials to be less reactive with CO_2, and this effect has been more significant for BGC. Previous studies have reported that rapid devolatilization could promote the char gasification characteristics due to the accelerated release of the volatile matter, which can increase the internal pressure of pores and destroy their structures to increase the specific surface area [35], [36]. However, the rapid devolatilization at high temperatures (e.g.,1500 °C) reduces the chemical functional groups and increase the ash content, while the carbonaceous materials ranking is upgraded (e.g., fixed caron and energy content increased). This results in more compact stable structures hindering the char gasification [20]. The reactivity index for

all three chars produced by rapid devolatilization process at 1500 °C was lower than that for the raw carbonaceous materials with the index ratio for BGC 1500 °C, TC 1500 °C and CC 1500 °C being 84.21%, 92.11% and 94.23% of their raw materials respectively.

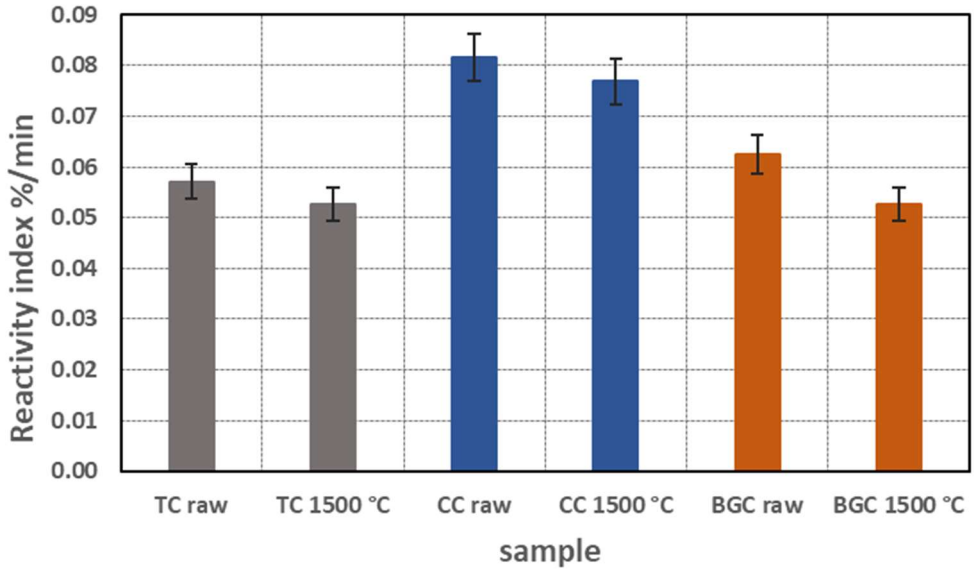

Figure 5. Reactivity index for raw materials and devolatilized chars produced under rapid heating at 1500 °C.

The results in Figure 5 further confirm that CC will be the most reactive carbonaceous material in HIsarna SRV, while TC and BGC have very similar gasification behaviour. The higher reactivity for CC may cause instability in the SRV due to behaviours such as foaming from faster CO formation and changes in furnace temperature, and may lead to lower efficiency in SRV, therefore it is necessary to enhance the productivity of the CCF during CC injection to utilize the extra CO generated from the CC devolatilization.

3.3. Qualitative SEM analysis

SEM images of all three raw materials and their chars produced from rapid devolatilization at 1500 °C are shown in Figures 6. These images represent a bulk behaviour for each carbonaceous material. furthermore, an individual particle from each material before and after rapid devolatilization is magnified for an in-depth study and represented in Figures 7 and 8 respectively.

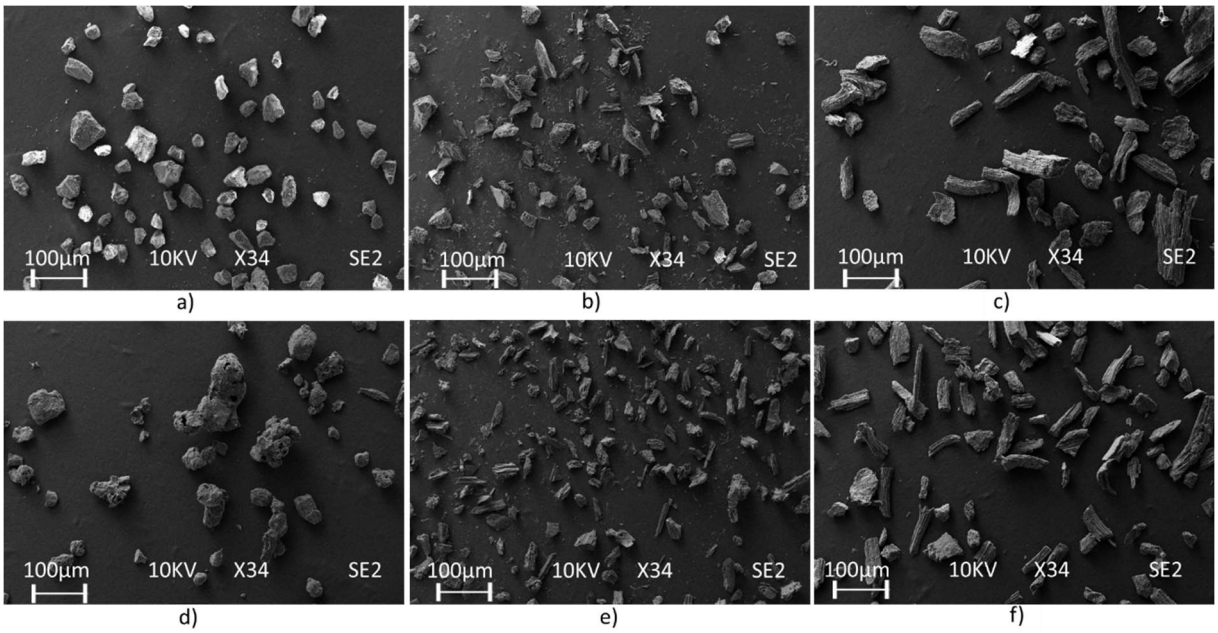

Figure 6. *SEM images of bulk materials (a) TC raw; (b) CC raw; (c) BGC raw; (d) TC 1500°C; (e) CC 1500 °C; and (f) BGC 1500 °C.*

Comparison of these chars from rapid devolatilization and their corresponding parent materials shows significant morphological changes caused by the rapid devolatilization process. These images are taken after a preliminary analysis of a large sample to ensure that typical morphologies observed for each sample. The difference in size, shape and surface roughness can be noticed for parent materials and their chars produced from rapid devolatilization. The TC particles are observed very compact with irregular shape and smooth and non-porous surface as can be seen in Fig. 7a. However, both biomass samples (CC and BGC) have maintained their fibrous structure, and the cross-section view of CC shows that the capillaries from the wood are still present with a large number of micropore and mesopores of non-uniform size on the plane surface which will contribute to the relatively larger specific surface for CC as shown in Fig. 7b. Less capillaries of small diameter and coarser particle surface can be observed through the BGC particle (Fig. 7c).

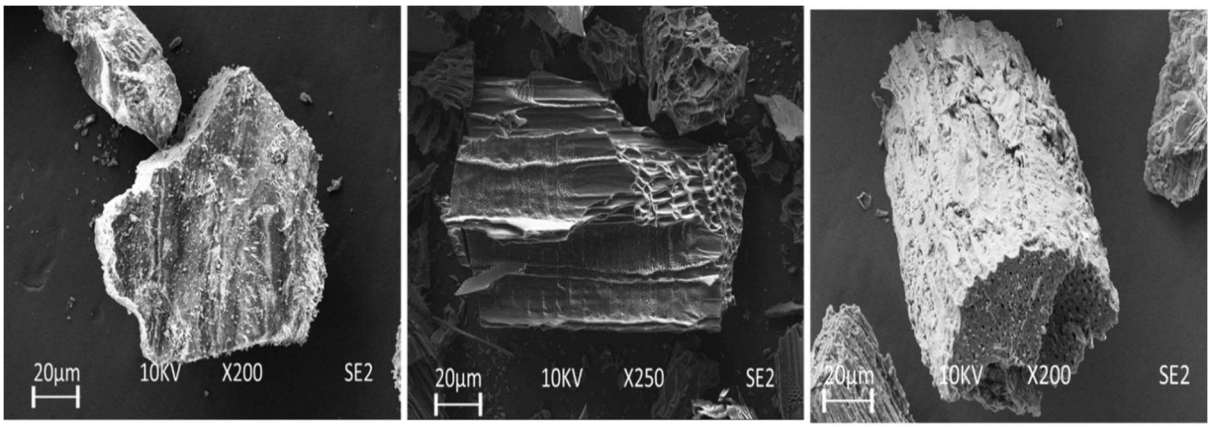

Figure 7. SEM images of raw materials (a) Thermal coal TC (b) Charcoal CC (c) Bana grass char BGC

The oblong particles observed for BGC with the length of the particle is larger than the sieve range (90-300 µm) used. During sieving process only the width of the particle is considered, since oblong particles may pass through the mesh with its minor size, as a result the representative size is much higher than it is counted for, which has also been reported by other researchers [37]. In contrast, CC is the mixture of more irregular shape with some spherical and oblong particles.

As it can be noted in Figure 8 all the char particles produced from rapid heating at 1500 °C maintained similar shapes to their parent materials, however the size of the char particles is reduced compared to the parent materials, although some of the particles are sintered for TC. This change can be linked to mechanisms such as particle shrinking or fragmentation depending on the thermal treatment. Both biomass samples were able to maintain the morphology similar to their parent materials, because the natural porosity within the materials allows the release of the volatile products without severe change in the particle structure. In contrast, TC sample has gone through much more severe transformation, as it can be seen in Fig. 8a, large openings on the char surface are observed, which are caused by the release of volatile products through a melting surface of the char during the rapid devolatilization at 1500 °C.

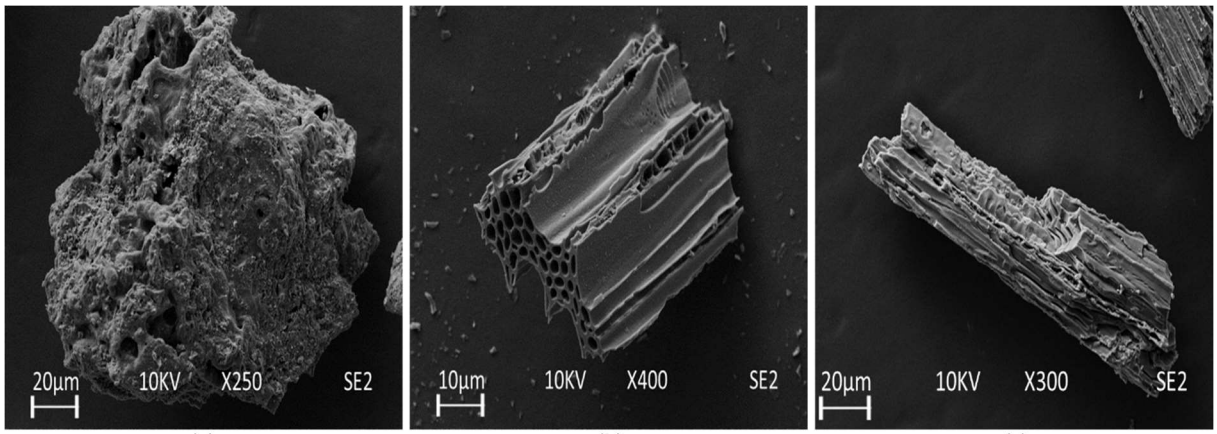

Figure 8. SEM images of chars produced from rapid devolatilization at 1500 °C for (a) Thermal coal TC (b) Charcoal CC (c) Bana grass char BGC.

During the rapid heating, the solid matrixes of carbonaceous materials are softened, resulting in some of the pores to be clogged. Then the volatile matters generated inside the particle creates an overpressure, which leads to bubbles formation and subsequently burst to the openings on the char surface [12]. This phenomena is more evident in the TC particle due to more compact structure and thermal coal also known to have higher thermoplasticity [38], as a result swelled surfaces and large cavities under the surface can be seen in Fig. 8a. It can be speculated that this behaviour in TC particle can create smoother surface, which can cause the material to be less reactive for the subsequent steps of oxidation. Although the chars of CC and BGC after rapid devolatilization retained their parental shapes, this rapid heating is likely to have caused collapsing phenomena due to melting of ash and softening in the solid matrix, as a result more compact structure has been produced than their parental materials. This explains the slowdown in the gasification behaviour during the reactivity tests for all carbonaceous materials, BGC with the highest ash content is expected to suffer the most, followed by TC and CC as shown in Fig. 4 and Fig.5.

3.4 Quantitative BET analysis

The porosities of the raw carbonaceous materials and their chars produced by the rapid devolatilization at 1500 °C are measured by the N_2 adsorption–desorption isotherms and shown in Fig. 8. According to the International Union of Pure and Applied Chemistry (IUPAC) classifications the

isotherms for both TC and TC 1500 °C belong to type III isotherm as can be seen in Figs. 9a &9d respectively. The flat region corresponds to the monolayer formation, which indicates weak interaction between the adsorbent-adsorbate, and this could be due to non-porous or existent of macroporous only on the TC structure [39]. The rapid devolatilization caused the adsorption isotherm to increase slightly for TC, and it has resulted in an increase in the average pore diameter and BET surface area as shown in Table 2. The adsorption isotherms for both CC raw and BGC raw shown in Figs. 9b & 9c belong to type I isotherm, which indicate more microporous in these materials [40]–[42]. Also for both materials steep uptake is visible at very low p/p_0, which is due to high interactions between adsorbent-adsorbate in narrow micropores as a result micropores are filled at very low p/p_0 [39].

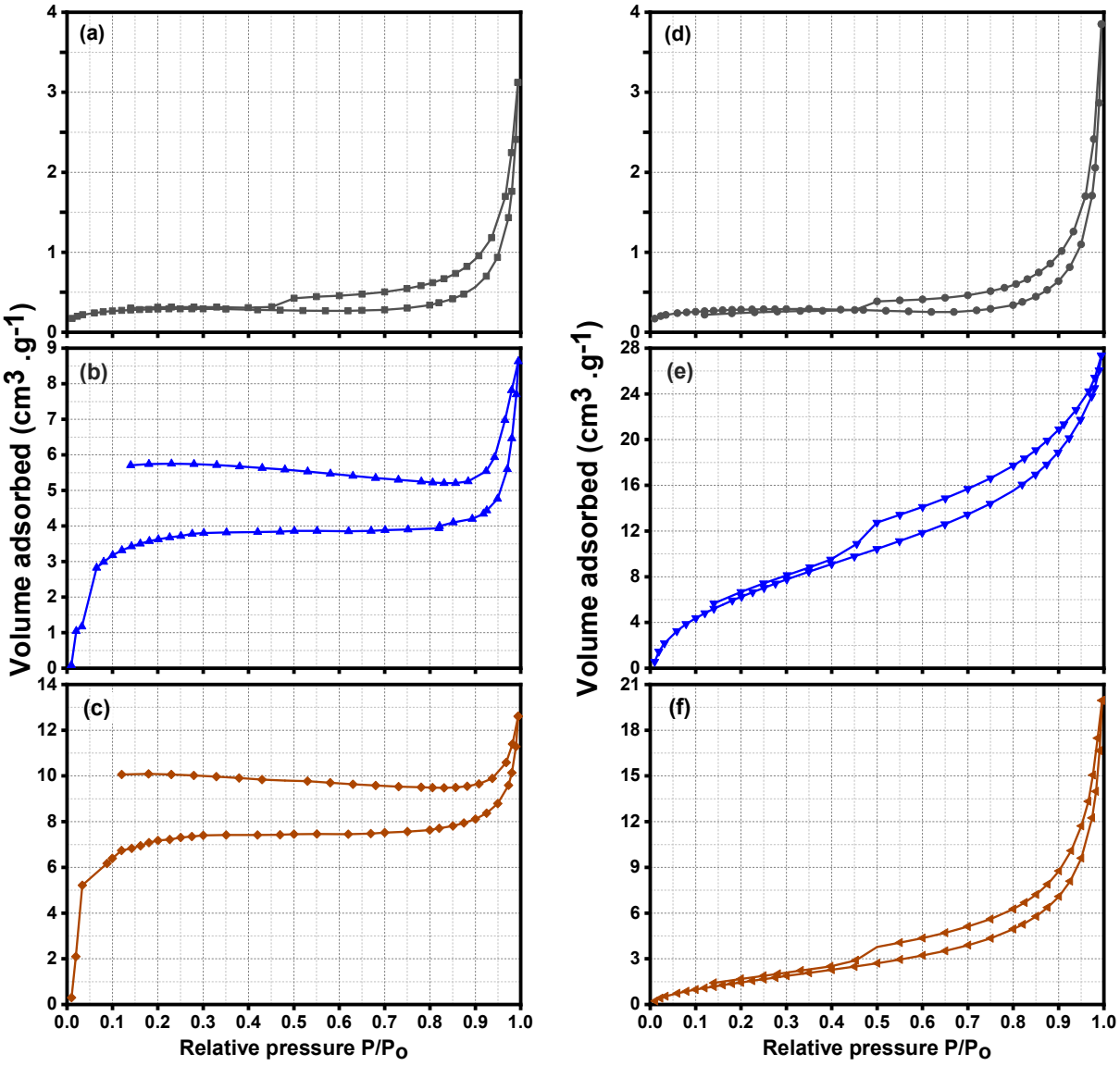

Figure 9. Nitrogen adsorption–desorption isotherms of (a) TC raw; (b) CC raw; (c) BGC raw; (d) TC 1500°C; (e) CC 1500 °C; (f) BGC 1500 °C.

As shown in Figs. 9e and 9f, both CC 1500 °C and BGC 1500 °C belong to type II isotherm, which confirms changes in the pore structure for both materials under the rapid heating [39]. Although steeper uptake is visible for the BGC raw compared to the CC raw at low p/p_0, the isotherm for CC 1500 °C (Fig. 9e) is significantly steeper than the isotherm for BGC 1500 °C (Fig. 9f) at low p/p_0. This could be due to higher collapsing of micropores in BGC compared to CC from the results of higher ash content in the BGC which can melt and soften the solid matrix during the rapid heating at 1500 °C. As it can be seen in Figs. 9b & 9c, both CC and BGC raw isotherms present a non-reversible desorption branch, and this is due to presence of constricted micropores which limits the adsorption of the N_2 at 77K. In contrast, all the other materials including CC 1500 °C and BGC 1500 °C produced a hysteresis loop at the relative pressure between 0.45 and 0.99. Similar findings has been reported by Wang et al. [43] which has been linked to the difference in the evaporation behaviour compared to condensation within the pores due to capillary condensation in mesopores.

The BET surface area, pore volume and average pore diameter determined are shown in Table 2 for all three raw materials and their chars after the rapid heating at 1500 °C. Despite the slight increase in the BET surface area and average pore diameter after rapid devolatilization, both TC raw and TC 1500 °C appear to have significantly smaller surface area compared to the biomass materials, which results in the lower reaction rate for the TC samples. As expected, CC raw has very large surface area that was further increased by the rapid devolatilization, while the average pore diameter decreased significantly. This could be due to particle fragmentation during the rapid heating resulting in the smaller particles and high surface area, subsequently larger amount of N_2 adsorbed while the average pore diameter decreased which could be due to blockage or collapse of some of the original pores [42].

Table 2. BET surface area and pore characteristic parameters for both raw carbonaceous materials and chars produced during rapid devolatilization at 1500 °C.

Samples	BET Surface area[a] /$m^2\,g^{-1}$	Pore volume[b] /cm^3g^{-1}	Average Pore diameter[c] /Å

TC raw	1.1	0.004	216.7
TC 1500 °C	1.5	0.005	249.0
CC raw	36.0	0.025	459.8
CC 1500 °C	61.7	0.060	52.7
BGC raw	48.6	0.032	553.5
BGC 1500 °C	13.4	0.030	111.4

414 [a]BET equation was applied between p/p_0=0.05-0.3 at adsorption branch of the isotherm. [b]Total pore
415 volume at p/p_0=0.99. [c]Desorption average pore width by BJH method.

416 BGC raw appears to have higher BET surface area compared to other raw materials, but the BET
417 surface area and average pore diameter decreased quite significantly by the rapid heating. This
418 behaviour in BGC again could be due to the high ash content, ash composition and morphology in the
419 BGC raw and the ash in BGC raw material will melt during the rapid heating and create more compact
420 structure with smaller surface, hence this is also evident in the gasification tests. These BET results
421 illustrate that gasification behaviour of carbonaceous materials may be controlled more by
422 parameters such as particle shape, porosity, ash content and chemistry rather than the surface area
423 for the materials selected for this study.

424 **3.5. Temperature effect on char size and shape variation**

425 It is apparent from Figures 7 & 8 that rapid devolatilization results in changes in size and shape of the
426 carbonaceous materials caused by the release of the large amount of volatile products in a short
427 period of time. The size and shape of the solid carbonaceous materials may play an important role in
428 the HIsarna reactor due to their effects on the fluid dynamics and the diffusion mechanisms. To better
429 understand the variation in size and shape under thermal treatment, the high temperature confocal
430 laser scanning microscope (HT-CSLM) has been applied. The main advantage of using this technique is
431 that HT-CSLM allows continuous imaging of 2D plane of particles at the temperature under controlled
432 high heating rate (up to 100 °C/min) while the changes in the size and shape are taking place. Figure
433 10 shows the comparison of the average change in the particle size and shape for all the parent
434 carbonaceous materials studied. The results show that the final swelling ratio for all materials is

smaller than 1, which confirms that devolatilization results in decrease in the particle size for all the materials.

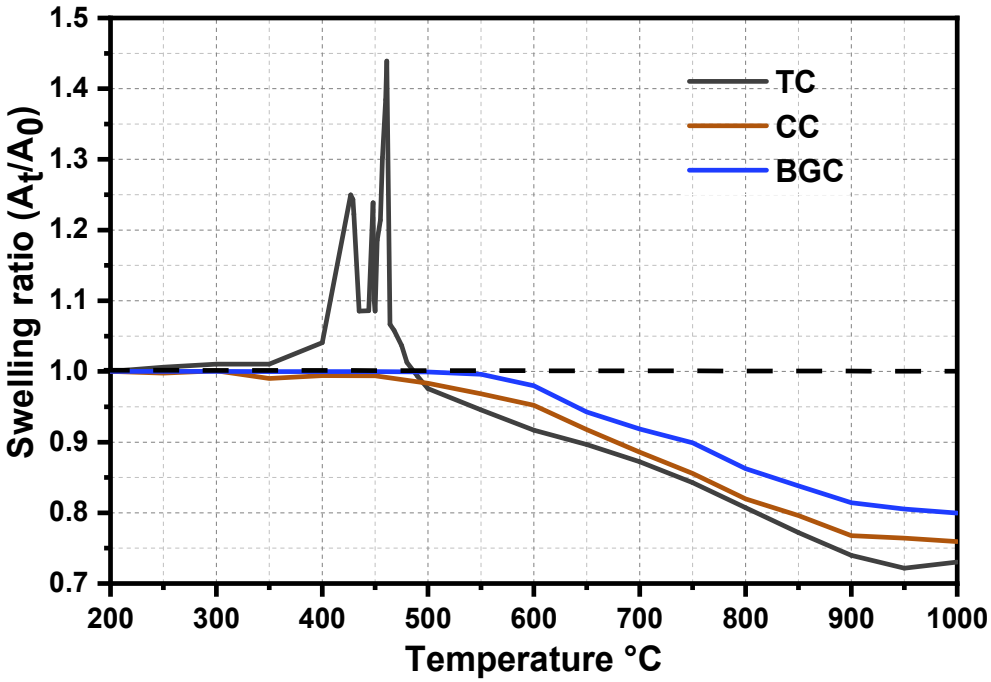

Figure 10. A comparison of an average swelling profile for five particles of each raw carbonaceous material under argon at heating rate of 100 °C/min in the HT-CSLM.

The swelling ratio profile for TC shows that at the temperature between 380 °C and 470 °C the swelling ratio increases in a series of oscillation. This behaviour in TC can be linked to the formation and rupture of bubbles due to the release of volatile products and reformation of bubbles within that temperature range as shown in Figs. 11b to 11d. This phenomenon is most obvious in particle one and particle five which are highlighted. It is believed that this variation in the swelling profile in that temperature range is attributed to the release of different volatile products due to decomposition of different components at a specific temperature. This behaviour agrees with the authors' previous findings for the same thermal coal material, which shows that each volatile products such as CO, CO_2, H_2 and light hydrocarbons is released at specific temperatures within the temperature range between 400 °C and 500 °C during thermal decomposition [44]. After reaching the maximum swelling ratio at 460 °C the reformation of bubbles no longer takes place, and the particle size decreases rapidly due to severe bubble ruptures and particle shrinking. As a result, the average particle size is reduced to around 72%

of the particles' starting surface area, which proves that higher degree of transformation (i.e., structural change) takes places in TC than biomass samples.

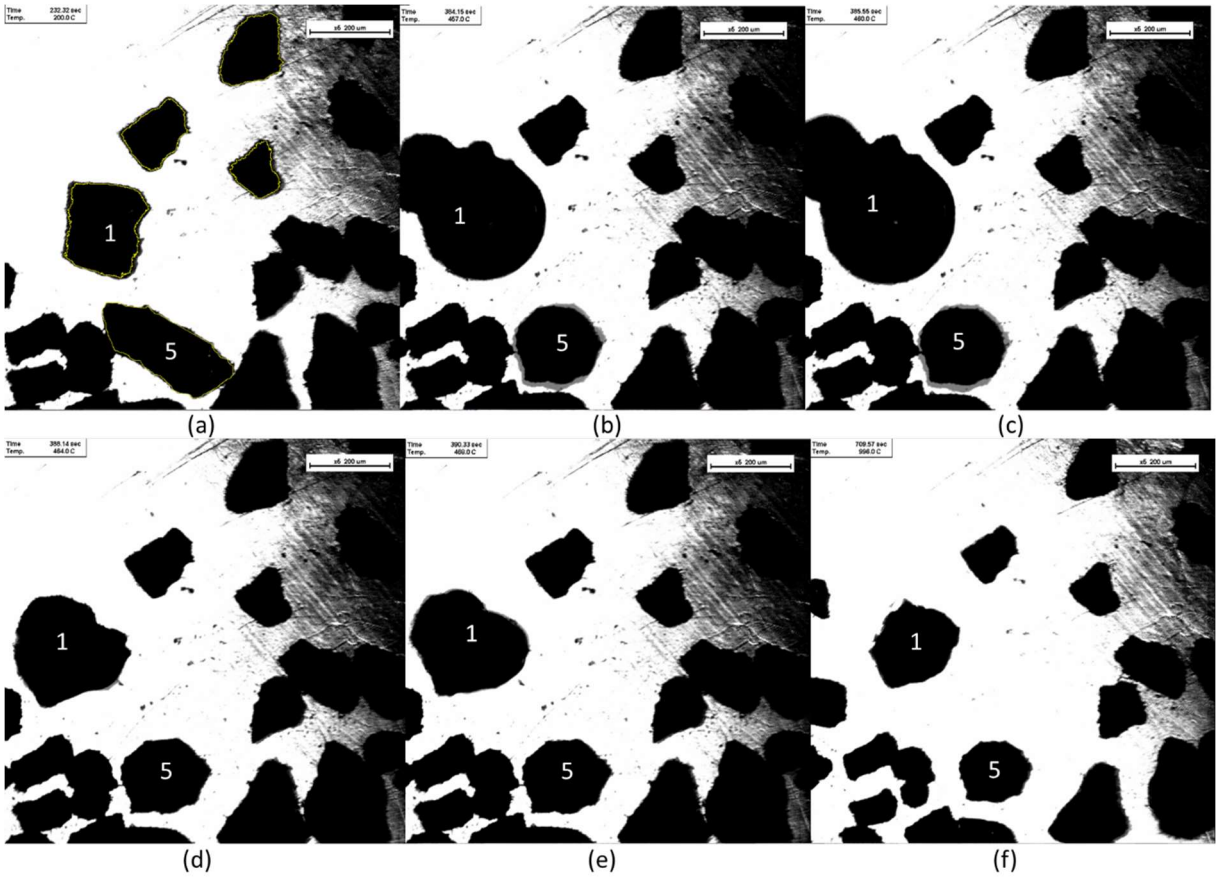

Figure 11. Illustration of swelling behaviour of TC at (a) 200 °C; (b) 457 °C; (c) 460 °C; (d) 464 °C; (e) 468 °C; and (f) 996 °C during heating in the HT-CSLM at 100 °C/min.

The behaviour of biomass samples (CC and BGC) differs from that observed for TC. No swelling was observed for either biomass sample, but the particle size for both materials was observed to decrease. The decrease in the swelling profile starts at different temperatures for each biomass sample. The decrease in the average particle size for CC starts at temperature around 350 °C, at a very slow ratio but it accelerates at the temperature > 450 °C with the final particle size being around 76% of starting particle. Again this result agrees with previous finding by the authors on devolatilization behaviour for the same material, and this confirm the size decrease is due to release of volatiles and reactions at the particle surface [44]. The decrease in the swelling ratio for BGC was observed to start at the temperature >550 °C, this could be related to the fact that BGC has already been pre-treated to 500

°C during production and as such lower molecular weight/lower boiling point volatiles may have already undergone some devolatilization.

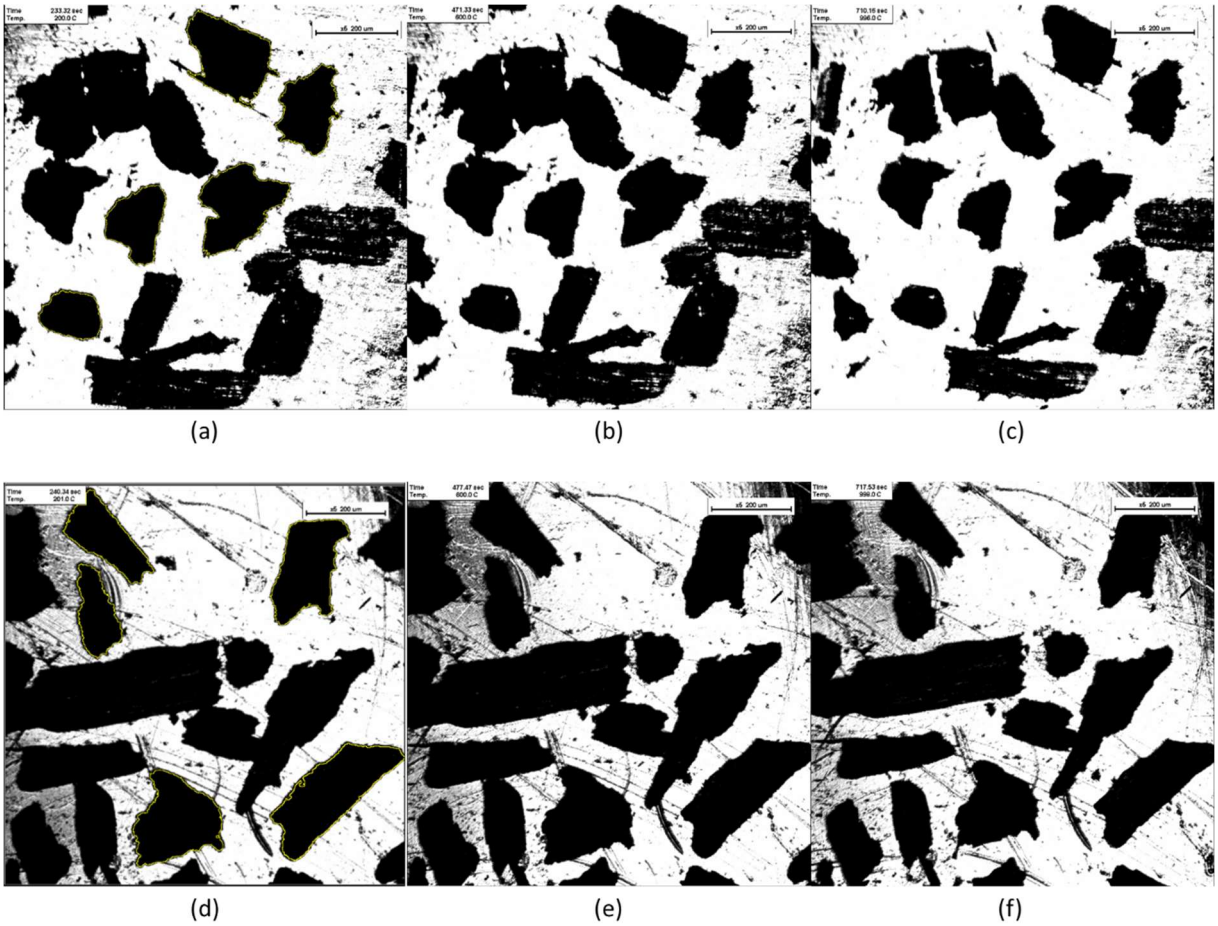

Figure 12. Illustration of changes in particle size and shape of CC at (a) 200 °C; (b) 600 °C; (c) 996 °C; and BGC at (d) 200 °C; (e) 600 °C; and (f) 998 °C.

The final average particle size for BGC was reduced to 80% of the starting particle size. Furthermore, there is no change in shape of biomass samples, and both CC and BGC retained the shapes of their parental materials, but TC particles suffered much more severe physical changes and the particle roundness increased.

4. Conclusion

To understand the behaviour of carbonaceous materials during injection in the novel HIsarna ironmaking process, chars of three different carbon sources are produced by rapid devolatilization at 1500 °C which is similar to the thermal conditions the injected carbonaceous materials undergo in the HIsarna process. The behaviours (reactivity, morphology change, surface area and swelling) of three

different carbon sources and their chars produced from rapid devolatilization at 1500 °C were investigated using analytical and morphological methods. The following conclusions can be drawn from this study:

- CC has gone through the highest carbon conversion degree (X) during rapid devolatilization, followed by TC and BGC, 30.1%, 22.0% and 19.8% respectively. This confirms that the devolatilization conversion is not determined by the volatile matter (VM) content only, but the physical and chemical properties of the carbonaceous materials also directly influence the conversion degree during rapid devolatilization.
- CC has shown the fastest gasification reaction before and after rapid devolatilization, followed by BGC raw and TC raw. Rapid devolatilization caused the chars produced from all materials to be less reactive with CO_2, but this behaviour was more significant for BGC. As a result, both TC 1500 °C and BGC 1500 °C have shown very similar gasification reaction.
- Rapid devolatilization resulted in the decreased particle size for all carbonaceous materials due to the release of volatiles and fragmentation. SEM images showed that chars produced from TC have gone through severe degree of structural transformation while chars from biomass samples (CC and BGC) maintained their parent structural shapes. This is confirmed by the direct observation of the structural change for all three carbonaceous materials using HT-CSLM.
- The BET results indicate that TC is non-porous or contains macroporous only, while both raw biomass samples (CC and BGC) contain a large number of constricted micropores and mesopores which resulted in significantly larger surface area for biomass samples. However, the average pore diameter decreased significantly for both CC and BGC because of rapid heating leading to blockage or collapse of some of the original pores. Furthermore, the gasification reaction is controlled more by parameters such as particle shape, porosity, ash content and chemistry rather than the surface area.

Acknowledgement

DK would like to thank Tata Steel Nederland Technology BV for providing the PhD scholarship (Reference No: COL1421/GIPS03241) to carry out this research. ZL would like to appreciate the funding from EPSRC under the grant number EP/N011368/1. The authors appreciate Tata Steel HIsarna team for fruitful discussions and providing samples. DK gratefully acknowledges the kind support by Dr. Stephen Spooner at Swansea University for HT-CSLM training.

References

[1] K. Meijer, C. Zeilstra, C. Teerhuis, M. Ouwehand, and J. Van Der Stel, "Developments in alternative ironmaking," *Trans. Indian Inst. Met.*, 2013, doi: 10.1007/s12666-013-0309-z.

[2] J. W. K. Van Boggelen, H. K. A. Meijer, C. Zeilstra, H. Hage, and P. Broersen, "HIsarna - Demonstrating low CO 2 ironmaking at pilot scale," no. September 2018, pp. 25–27, 2018.

[3] K. Meijer, C. Guenther, and R. J. Dry, "HIsarna Pilot Plant Project," *InSteelCon*, no. July, pp. 1–5, 2011.

[4] L. Ab, *HIsarna Experimental Campaigns B and C*, vol. 9424. 2013.

[5] F. N. H. Schrama, E. M. Beunder, J. W. K. van Boggelen, R. Boom, and Y. Yang, "Desulphurisation of HIsarna hot metal - a comparison study based on plant data," *Sci. Technol. Ironmak. Steelmak.*, pp. 419–422, 2017.

[6] I. J. Van Der Stel and K. Meijer, "Update to the Developments of Hisarna An Ulcos alternative ironmaking process," no. November, 2013.

[7] Z. Chen, C. Zeilstra, J. van der Stel, J. Sietsma, and Y. Yang, "Review and data evaluation for high-temperature reduction of iron oxide particles in suspension," *Ironmak. Steelmak.*, vol. 0, no. 0, pp. 1–7, 2019, doi: 10.1080/03019233.2019.1589755.

[8] Y. Qu, Y. Yang, Z. Zou, C. Zeilstra, K. Meijer, and R. Boom, "Thermal decomposition behaviour of fine iron ore particles," *ISIJ Int.*, vol. 54, no. 10, pp. 2196–2205, 2014, doi: 10.2355/isijinternational.54.2196.

[9] Y. Qu, Y. Yang, Z. Zou, C. Zeilstra, K. Meijer, and R. Boom, "Kinetic study on gas molten particle reduction of iron ore fines at high temperature," *Ironmak. Steelmak.*, vol. 42, no. 10,

pp. 763–773, 2015, doi: 10.1179/1743281215Y.0000000021.

[10] Y. Cheng, B. H. Yan, C. X. Cao, Y. Cheng, and Y. Jin, “Experimental investigation on coal devolatilization at high temperatures with different heating rates,” *Fuel*, vol. 117, no. PARTB, pp. 1215–1222, 2014, doi: 10.1016/j.fuel.2013.08.016.

[11] E. Biagini, A. Fantei, and L. Tognotti, “Effect of the heating rate on the devolatilization of biomass residues,” *Thermochim. Acta*, vol. 472, no. 1–2, pp. 55–63, 2008, doi: 10.1016/j.tca.2008.03.015.

[12] E. Biagini, M. Simone, and L. Tognotti, “Characterization of high heating rate chars of biomass fuels,” *Proc. Combust. Inst.*, vol. 32 II, no. 2, pp. 2043–2050, 2009, doi: 10.1016/j.proci.2008.06.076.

[13] S. L. TEASDALE and P. C. HAYES, “Kinetics of Reduction of FeO from Slag by Graphite and Coal Chars,” *ISIJ Int.*, vol. 45, no. 5, pp. 642–650, 2005, doi: 10.2355/isijinternational.45.642.

[14] X. A. Huang, K. W. Ng, L. Giroux, and M. Duchesne, “Carbonaceous Material Properties and Their Interactions with Slag During Electric Arc Furnace Steelmaking,” *Metall. Mater. Trans. B Process Metall. Mater. Process. Sci.*, vol. 50, no. 3, pp. 1387–1398, 2019, doi: 10.1007/s11663-019-01569-1.

[15] S. L. Teasdale and P. C. Hayes, “Kinetics of reduction of FeO from slag by graphite and coal chars,” *ISIJ Int.*, vol. 45, no. 5, pp. 642–650, 2005, doi: 10.2355/isijinternational.45.642.

[16] J. K. Wright and B. R. Baldock, “Dissolution kinetics of particulate graphite injected into iron/carbon melts,” *Metall. Trans. B*, vol. 19, no. 2, pp. 375–382, 1988, doi: 10.1007/BF02657735.

[17] R. Khanna, F. McCarthy, H. Sun, N. Simento, and V. Sahajwalla, “Dissolution of carbon from coal-chars into liquid iron at 1550°C,” *Metall. Mater. Trans. B Process Metall. Mater. Process. Sci.*, vol. 36, no. 6, pp. 719–729, 2005, doi: 10.1007/s11663-005-0075-3.

[18] S. Tsuey Cham, “Investigating Factors that Influence Carbon Dissolution from Coke into Molten Iron,” no. February, 2007, [Online]. Available: internal-pdf:/S. Tsuey

Cham_02whole_encrpt.pdf

[19] J. Yu, J. A. Lucas, and T. F. Wall, “Formation of the structure of chars during devolatilization of pulverized coal and its thermoproperties: A review,” *Prog. Energy Combust. Sci.*, vol. 33, no. 2, pp. 135–170, 2007, doi: 10.1016/j.pecs.2006.07.003.

[20] K. Zhang, Z. Wang, W. Fang, Y. He, E. Hsu, Q. Li, J. Gul-e-Rana, and K. Cen, “High-temperature pyrolysis behavior of a bituminous coal in a drop tube furnace and further characterization of the resultant char,” *J. Anal. Appl. Pyrolysis*, vol. 137, no. August 2018, pp. 163–170, 2019, doi: 10.1016/j.jaap.2018.11.022.

[21] E. Biagini, P. Narducci, and L. Tognotti, “Size and structural characterization of lignin-cellulosic fuels after the rapid devolatilization,” *Fuel*, vol. 87, no. 2, pp. 177–186, 2008, doi: 10.1016/j.fuel.2007.04.010.

[22] A. Smolínski and N. Howaniec, “Analysis of porous structure parameters of biomass chars versus bituminous coal and lignite carbonized at high pressure and temperature-A chemometric study,” *Energies*, vol. 10, no. 10, pp. 28–30, 2017, doi: 10.3390/en10101457.

[23] J. Tanner and S. Bhattacharya, “Kinetics of CO2 and steam gasification of Victorian brown coal chars,” *Chem. Eng. J.*, vol. 285, pp. 331–340, 2016, doi: 10.1016/j.cej.2015.09.106.

[24] O. Karlström, A. Brink, E. Biagini, M. Hupa, and L. Tognotti, “Comparing reaction orders of anthracite chars with bituminous coal chars at high temperature oxidation conditions,” *Proc. Combust. Inst.*, vol. 34, no. 2, pp. 2427–2434, 2013, doi: 10.1016/j.proci.2012.07.011.

[25] J. Li, G. Bonvicini, L. Tognotti, W. Yang, and W. Blasiak, “High-temperature rapid devolatilization of biomasses with varying degrees of torrefaction,” *Fuel*, vol. 122, pp. 261–269, 2014, doi: 10.1016/j.fuel.2014.01.012.

[26] W. H. Chen, S. W. Du, and T. H. Yang, “Volatile release and particle formation characteristics of injected pulverized coal in blast furnaces,” *Energy Convers. Manag.*, vol. 48, no. 7, pp. 2025–2033, 2007, doi: 10.1016/j.enconman.2007.01.001.

[27] G. Newalkar, K. Iisa, A. D. Damico, C. Sievers, and P. Agrawal, “Effect of temperature,

584 pressure, and residence time on pyrolysis of pine in an entrained flow reactor," *Energy and*
585 *Fuels*, vol. 28, no. 8, pp. 5144–5157, 2014, doi: 10.1021/ef5009715.
586 [28] I. A. Moore, "Direct Observation of Swelling Coal Particles," no. October, 2018.
587 [29] K. H. van Heek and W. Hodek, "Structure and pyrolysis behaviour of different coals and
588 relevant model substances," *Fuel*, vol. 73, no. 6, pp. 886–896, 1994, doi: 10.1016/0016-
589 2361(94)90283-6.
590 [30] Y. Qiao, S. Chen, Y. Liu, H. Sun, S. Jia, J. Shi, C. M. Pedersen, Y. Wang, and X. Hou, "Pyrolysis of
591 chitin biomass: TG-MS analysis and solid char residue characterization," *Carbohydr. Polym.*,
592 vol. 133, pp. 163–170, 2015, doi: 10.1016/j.carbpol.2015.07.005.
593 [31] E. Biagini, S. Pintus, and L. Tognotti, "Characterization of high heating-rate chars from
594 alternative fuels using an electrodynamic balance," *Proc. Combust. Inst.*, vol. 30 II, no. 2, pp.
595 2205–2212, 2005, doi: 10.1016/j.proci.2004.07.005.
596 [32] W. H. Chen, S. W. Du, C. H. Tsai, and Z. Y. Wang, "Torrefied biomasses in a drop tube furnace
597 to evaluate their utility in blast furnaces," *Bioresour. Technol.*, vol. 111, pp. 433–438, 2012,
598 doi: 10.1016/j.biortech.2012.01.163.
599 [33] S. B. Liaw and H. Wu, "A New Method for Direct Determination of Char Yield during Solid Fuel
600 Pyrolysis in Drop-Tube Furnace at High Temperature and Its Comparison with Ash Tracer
601 Method," *Energy and Fuels*, vol. 33, no. 2, pp. 1509–1517, 2019, doi:
602 10.1021/acs.energyfuels.8b03161.
603 [34] D. Khasraw, S. Spooner, H. Hage, K. Meijer, and Z. Li, "Evaluation of devolatilization behaviour
604 of different carbonaceous materials under rapid heating for the novel HIsarna ironmaking
605 process," *Fuel*, vol. 292, no. December 2020, 2021, doi: 10.1016/j.fuel.2021.120329.
606 [35] Z. H. Wang, K. Zhang, Y. Li, Y. He, M. Kuang, Q. Li, and K. F. Cen, "Gasification characteristics
607 of different rank coals at H2O and CO2 atmospheres," *J. Anal. Appl. Pyrolysis*, vol. 122, pp.
608 76–83, 2016, doi: 10.1016/j.jaap.2016.10.019.
609 [36] S. Dong, P. Alvarez, N. Paterson, D. R. Dugwell, and R. Kandiyoti, "Study on the effect of heat

610 treatment and gasification on the carbon structure of coal chars and metallurgical cokes using
611 fourier transform raman spectroscopy," *Energy and Fuels*, vol. 23, no. 3, pp. 1651–1661,
612 2009, doi: 10.1021/ef800961g.
613 [37] T. J. Morgan, S. Q. Turn, A. George, and J. Aburto, "Fast pyrolysis behavior of banagrass as a
614 function of temperature and volatiles residence time in a fluidized bed reactor," *PLoS One*,
615 vol. 10, no. 8, 2015, doi: 10.1371/journal.pone.0136511.
616 [38] M. Fraga, B. Flores, E. Osório, and A. Vilela, "Evaluation of the thermoplastic behavior of
617 charcoal, coal tar and coking coal blends," *J. Mater. Res. Technol.*, vol. 9, no. 3, pp. 3406–
618 3410, 2020, doi: 10.1016/j.jmrt.2020.01.076.
619 [39] M. Thommes, K. Kaneko, A. V. Neimark, J. P. Olivier, F. Rodriguez-Reinoso, J. Rouquerol, and
620 K. S. W. Sing, "Physisorption of gases, with special reference to the evaluation of surface area
621 and pore size distribution (IUPAC Technical Report)," *Pure Appl. Chem.*, vol. 87, no. 9–10, pp.
622 1051–1069, 2015, doi: 10.1515/pac-2014-1117.
623 [40] V. Gargiulo, A. Gomis-Berenguer, P. Giudicianni, C. O. Ania, R. Ragucci, and M. Alfè,
624 "Assessing the Potential of Biochars Prepared by Steam-Assisted Slow Pyrolysis for CO2
625 Adsorption and Separation," *Energy and Fuels*, vol. 32, no. 10, pp. 10218–10227, 2018, doi:
626 10.1021/acs.energyfuels.8b01058.
627 [41] N. I. A. Ghani, N. Y. M. Yusuf, W. N. R. W. Isahak, and M. S. Masdar, "Modification of activated
628 carbon from biomass nypa and amine functional groups as carbon dioxide adsorbent," *J.*
629 *Phys. Sci.*, vol. 28, no. February, pp. 227–240, 2017, doi: 10.21315/jps2017.28.s1.15.
630 [42] T. Theint, Z. Yan, S. Spooner, V. Degirmenci, and K. Meijer, "Gasification and physical-
631 chemical characteristics of carbonaceous materials in relation to HIsarna ironmaking
632 process," *Fuel*, vol. 289, no. November 2020, p. 119890, 2021, doi:
633 10.1016/j.fuel.2020.119890.
634 [43] Z. Wang, Y. Cheng, Y. Qi, R. Wang, L. Wang, and J. Jiang, "Experimental study of pore
635 structure and fractal characteristics of pulverized intact coal and tectonic coal by low

temperature nitrogen adsorption," *Powder Technol.*, vol. 350, pp. 15–25, 2019, doi: 10.1016/j.powtec.2019.03.030.

[44] D. Khasraw, S. Spooner, H. Hage, K. Meijer, and Z. Li, "Devolatilisation characteristics of coal and biomass with respect to temperature and heating rate for HIsarna alternative ironmaking process," *Fuel*, vol. 284, no. July 2020, p. 119101, 2021, doi: 10.1016/j.fuel.2020.119101.